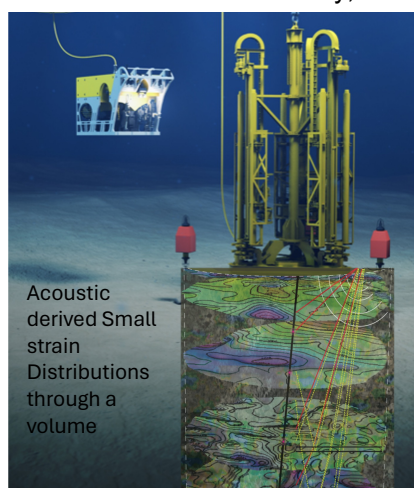


EXPERIMENTATIONS USING S-WAVE VELOCITIES AND ATTENUATIONS TO CORRELATE STRENGTH PROPERTIES ASSOCIATED WITH OFFSHORE WINDFARM DRILLING INTERACTIONS

J. Y. Guigné Acoustic Zoom Inc
J. Reyes-Montes Applied Seismology Consulting Ltd
G. Sutton MaREI Centre, University College Cork
J. Machin Subsea Micropiles (UK) Ltd.
J. Bentley Subsea Micropiles (UK) Ltd.

1 INTRODUCTION

Acoustic imaging is being directed to enable unprecedented high-resolution seismic beamforming of the geomechanical properties of the subseabed soils¹. It will mitigate risks to the offshore wind farm anchor design, increasing the quality of decision-making processes associated with installing infrastructure, which is required for challenging offshore seabed conditions. The approach reduces environmental risks to large-scale wind farm projects. It provides critical sub-seabed soil strength conditions unavailable today, essential for the foundation's efficient installation and operational



stability. It accelerates the completion of the development of offshore renewable energy projects at lower costs, with smaller carbon footprints and higher, less risky returns to investors. Subseabed foundation geotechnical properties, as distributed through a volume, will be acquired using the in-situ drill as a sound source while structural micropiles are installed into the seabed. The goal is to develop the acoustic imaging data acquisition and processing steps to enable the resulting piles to become "smart" linear receivers¹. This would enable the continuous characterization of the sub-seabed formation volume surrounding the micropile platform over the life of the field (See Figure 1). A new drill that transforms into a foundational micropile has been conceived. The drill's engineering has progressed into a new class of offshore hammer drills with shear wave imaging acquired and processed to advance the in-situ geotechnical information.

Figure 1 Subsea Micropile's Engineered Micropiling Drill on the seabed.

2 METHODOLOGY

Seismic velocity can be an effective parameter for characterizing the mechanical and hydrological properties of soils and rocks in the subsurface. Surface waves are dispersive when propagating in a vertical direction. As such, they can be used to map shear-wave velocities as a function of depth. Low-frequency surface waves can be used for profiling depths down to 30 metres for geotechnical applications. Profiling shallower depths (from 10's to a few 100 cm) requires using higher-frequency (shorter wavelength) surface waves.

In this experimental drilling study, the MASW (Multichannel analysis of surface waves) method was used based on spectral analysis of the Rayleigh waves to determine the seismic shear wave velocity profile as a function of depth. When rigorously applied, the MASW method can investigate the ground's elastic properties (stiffness) for geotechnical engineering and seismic hazard determination^{1,2,3,4}. Dispersion, or change in phase velocity with frequency, is the fundamental property in surface-wave methods^{1,2}. The phase velocity of the surface wave is sensitive to the shear

wave velocity (V_s); the phase velocity of the surface wave is typically 90-95% of the shear wave velocity^{2,3,5}. Surface wave dispersion can be significant in the presence of velocity layering, which is common in the near-surface environment^{6,7}.

Several classes of surface waves or waves travel along a surface². In this application, we focus exclusively on the Rayleigh wave, also called “ground roll,” since the Rayleigh wave is the dominant component of ground roll. The propagation of Rayleigh waves was modelled/monitored over a range of wavelengths at specified distances from the source. Group velocities were computed from the observed seismograms, from which the Rayleigh-wave dispersion characteristics and corresponding dispersion curves are derived. These curves show the behaviour of the phase and group velocities as a function of frequency for the different subsurface layers.

2.1 Experimental Program

From November 2023 into February 2024, a prototype drilling rig underwent a series of onshore drilling tests at the Jamestown Manufacturing site in Portarlinton, Co. Laois, Ireland, to prepare for offshore trials. The tests consisted of shallow drilling to a maximum depth of six meters. The trials used a nondestructive in-situ seismic technique and seismic refraction using P and S-wave arrivals for shallow subsurface imaging around the drilled boreholes. An initial 24-channel vertically responding geophone spread was deployed at the site to conduct a preliminary characterization of the energy propagating into the ground during drilling. Observations were made using two different geophone array configurations: first, with the drill at the crux of a 90-degree L shape with 12 geophones in each arm, and second, with the drill at one end of a single line with all 24 geophones. The frequency-time analysis of the passive monitoring, using the L-shaped array, showed an increase of three orders of magnitude (1000 times) in the vibration amplitude during drilling compared to background noise in the stations located within 6 m of the drill. This increase in amplitude was observed in a range of frequencies >40 Hz. A rapid decrease in amplitude was observed, with peak amplitudes decaying approximately 2 orders of magnitude within 40 m of the drill source.

The acoustic imaging used a 4kg hammer source between stations to provide a baseline depth profile of P and S-wave velocities to a depth of ~25 m (related to the total aperture of the monitoring array). The P-wave profile is a good reflection of the local lithology and showed a profile relatively undisturbed by the presence of the drill. On the other hand, the S-wave velocities showed a significant lateral variation caused by the drilling process, with perturbations observed to depths of 15-20 m. These changes in S-wave velocity, with increased values around the drill area, can be interpreted as a reflection of the degree of soil fluid changes, variable fracturing and fluid flow followed by loss of saturation, all induced by the drill during drilling. A further capture of returning images, using other surface wave phases, occurred by using the drill as the sound source and applying migration and stacking-based methods. A detailed image of the volume around the drill and the changes induced in the soil was acoustically observed by the process.

The attenuation of induced vibration was investigated by deploying a single-line array, with 24 vertical geophones spaced 3m, aligned between the drilling wellhead and outward. The results showed a rapid attenuation in Peak Particle Velocity (PPV) from the borehole source. An exponential attenuation with distance was measured, with 1.5 orders of magnitude decrease within 30 m of the borehole.

2.2 Data Acquisition System Used

During this study, an input force (source) is first provided by striking a hammer on a fibre plate, which excites a broad range of frequencies at amplitudes above the noise floor of the measuring system. In a second condition, drill hammering is used as a source as the drill descends into the ground, interacting with soil and bedrock (see Figure 2).



An array of seismic sensors (geophones in this case) connected to a data acquisition (DAQ) system located on the earth's surface records the seismic signals, from which a series of dispersion curves are produced and used to generate a profile of the shear-wave velocity as a function of depth (refer to Figure 3).

Figure 2 Subsea Micropile's Engineered Micropiling Drill onshore for the land shear wave velocity acoustic tests.

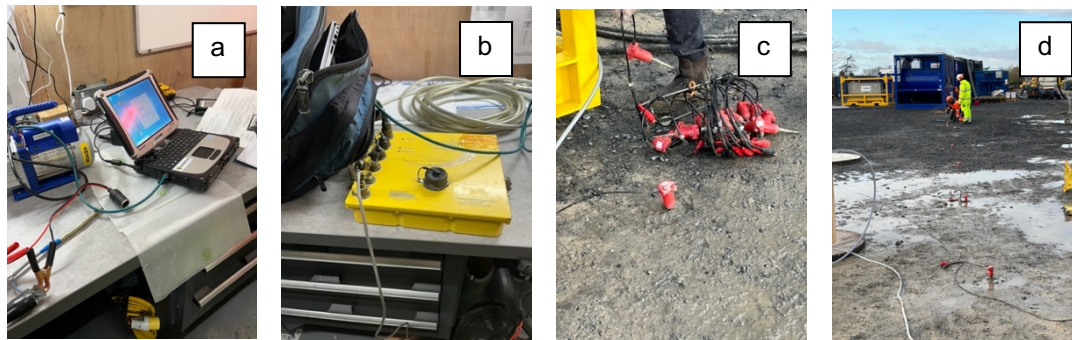


Figure 3 **a**-Data acquisition Laptop; **b**-Seismic Recorder; **c**-Line of 24 Geophones; **d**-placing the geophones around the drill site

3 DATA ANALYSIS AND RESULTS

3.1 Analysis

The impact of the drilling on the surrounding area was measured by recording the acoustic signal ahead of, during and after the drilling operations. The frequency-time analysis of records taken before the drilling, at the early stages of the drilling process and in the late stages of the borehole drill was analyzed. The results show an increase in amplitude of approximately three orders of magnitude in the range of frequencies > 40 Hz for the stations closest to the drill when operations are running.

These amplitudes decay towards the edges of the monitoring array, positioned 39 m from the drill by two orders of magnitude. Figure 4 shows Peak Particle Velocity (PPV) changes for sample pile driving hits with separation from the borehole source. An exponential attenuation with distance is observed, with a 1-order-of-magnitude decrease within 30 m of the borehole

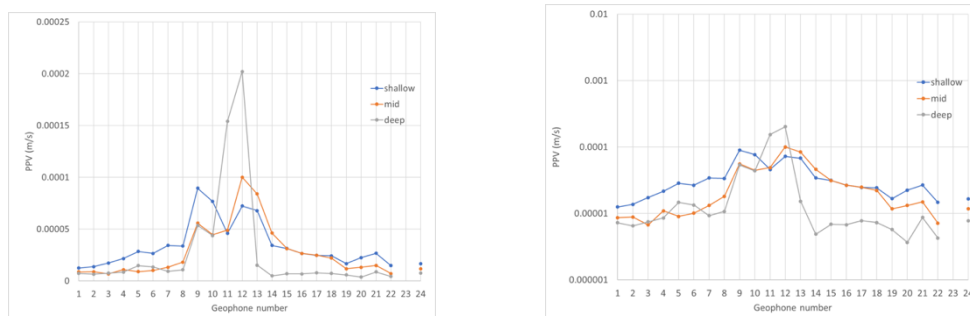


Figure 4 Peak Particle Velocity (PPV) measured for three different impacts at the drilling process at all geophones in the line: a: linear scale, b: log-lin scale.

Between geophone 12 and 13 indicates the position of the borehole.

3.2 Baseline Refraction Results

The recordings from the hammer hit surveys were inverted to calculate the velocity profiles along the lines for S-wave and P-wave transmission velocities (Figure 5 and Figure 6) using the seismic refraction method. The survey was carried out after the test borehole was drilled. Hammer hits were carried out at the central position between each pair of geophones and repeated 3 times at each position for enhanced signal-to-noise recordings after stacking. The results show that S-waves can provide a suitable resolution profile to a depth of ~25 m. The profile shows increased S-wave velocities around the drilled borehole up to a depth of 15m. These higher S-wave velocities could be associated with ground compaction or dewatering. The P-wave profile, shown in Figure 6, shows a depth profile relatively unaffected by the Drill or the drilling process, with the profile reflecting changes in lithology.

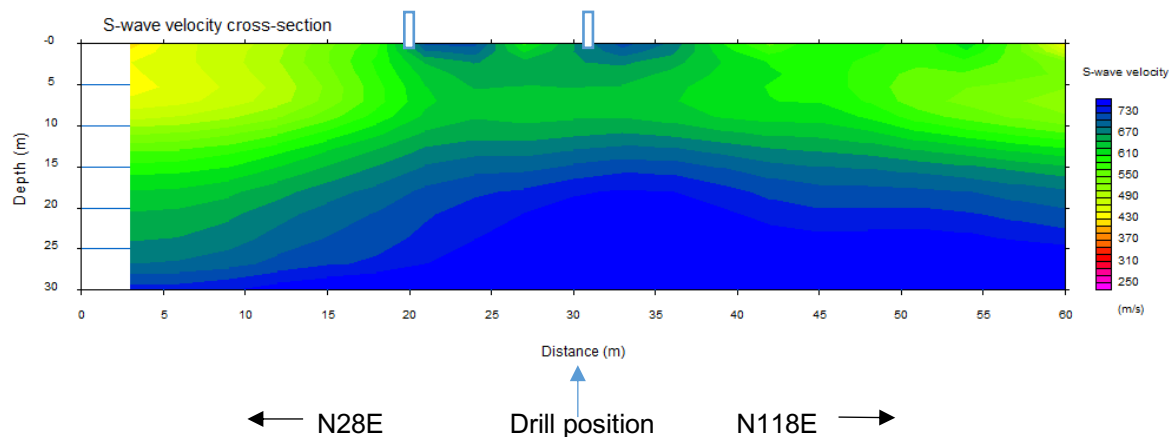


Figure 5 S-wave velocity profile calculated along the two lines of the L-shaped array. The white boxes indicate the projected position of the drilled borehole over the two profile lines.

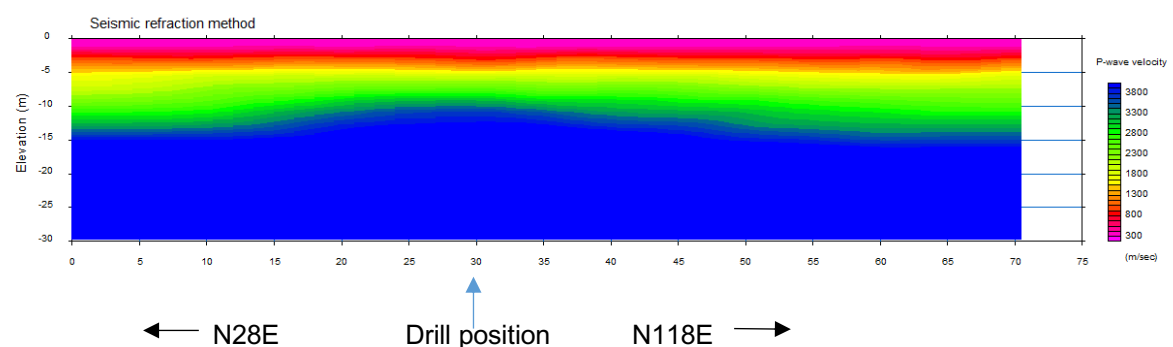


Figure 6 P-wave velocity profile calculated along the two lines of the L-shaped array. The white boxes indicate the projected position of the drilled borehole over the two profile lines.

3.3 Translating The Shear Wave Velocities To Soil Strength Parameters

S-wave velocities can be linked to geotechnical parameters and allow the characterization of the changes around the drilling site associated with the engineered micropiling drill footprint and the drilling process. Figures 7 and 8 present examples of such relationships in the literature.

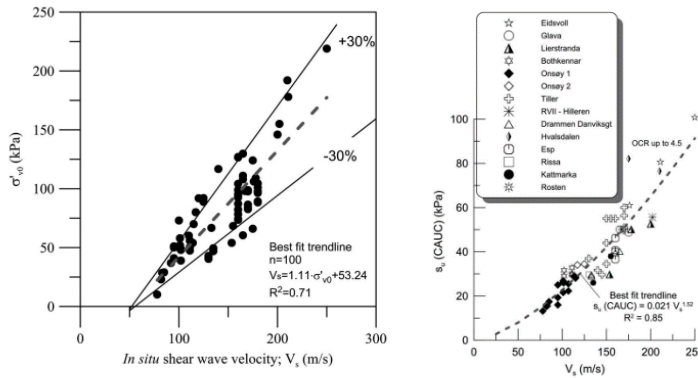


Figure 7 shows an example of the empirical correlation between S-wave velocity and geotechnical parameters in the literature, emphasizing vertical effective stress measured from high-quality samples of Norwegian clays⁸ and undrained shear strength from high-quality samples of Norwegian clays⁸.

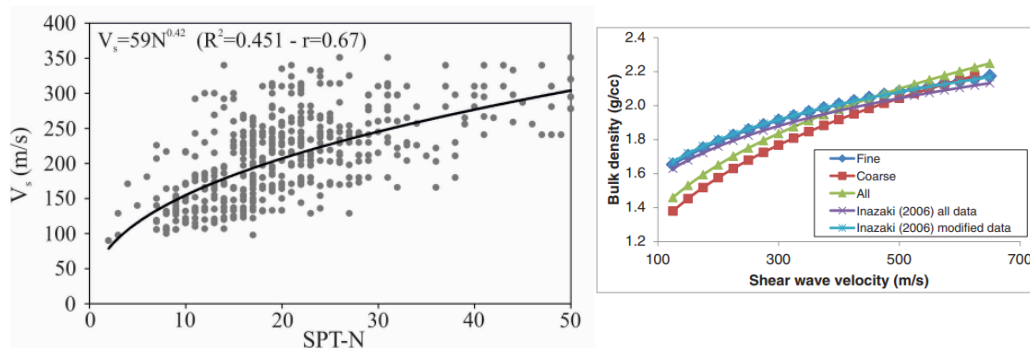


Figure 8 Example empirical correlations of SPT-N (associated with stiffness and friction angle)⁹ and bulk density for coarse and fine-grained soils¹⁰

Young's modulus and shear modulus characterize the stiffness of a material (e.g. rock or soil), representing the resistance against deformation along the stress axis or in shear. These can be calculated from the velocity of the seismic wave, particularly S-wave velocity, which is used as a direct indicator of material stiffness (refer to Figure 9) :

$$\text{Shear modulus } (\mu) = \rho V_s^2 ; \text{Young's modulus } (E) = \rho V_s^2 \frac{3 \left(\frac{V_p}{V_s} \right)^2 - 4}{\left(\frac{V_p}{V_s} \right)^2 - 1} = \rho V_s^2 (1 + \sigma) , \text{ where: } \rho: \text{medium}$$

density, Vs : S-wave velocity, Vp : P-wave velocity, σ : Poisson's ratio (typically assumed as 0.45 for soil or 0.3 for rock)

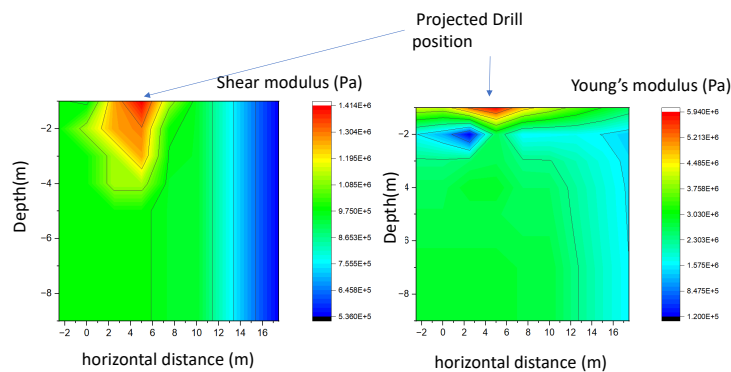


Figure 9 Resultant stiffness profiles using an average density for sandy-silty-clay soils of 2.65 cm³; stiffness moduli are computed from the profiles of seismic velocities

3.4 MASW Application in Time Using the Descending Drill as the Sound Source

The seismic traces from the 24 vertical channels were sampled at a frequency of 250 Hz, with a record length of 300 seconds. Record is treated as passive monitoring for MASW, with noise being the impact and vibration from the drill positioned at the array's centre. All the passive acquisition records were modified to obtain a series of records of 10 seconds in length. Signal data selection was made by examining the signals in the FK domain (removing spikes and equal energy repartition). Final data was extracted using a sliding window (grouping sequential channels 1-6, 2-7,...), producing a 1D S-wave profile at the centre of each window through dispersive pattern computation, first break picking and inversion.

Figure 10A shows a 10-second record highlighting the time histories and FK, Figure 10B illustrates an example of the resultant dispersion curve, and Figure 11 shows a 2D profile using the full drilling sequence to 5 m. depth, with its interpretation of soil stiffness shown in Figure 12. The moduli distribution after the full process shows low values in stiffness around the drill area, down to depths of ~10 m, that can be interpreted as water-saturated fractured zones accompanied by compaction in the region below depths of ~15 m within a 20 m radius of the drill.

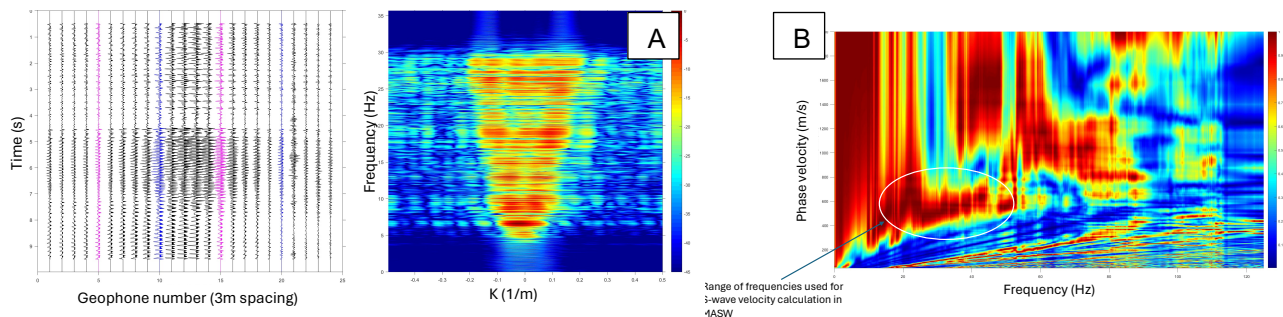


Figure 10 A 10-second record highlighting the time histories and FK and B the dispersion and range of frequencies used for S-wave velocity calculation in MASW

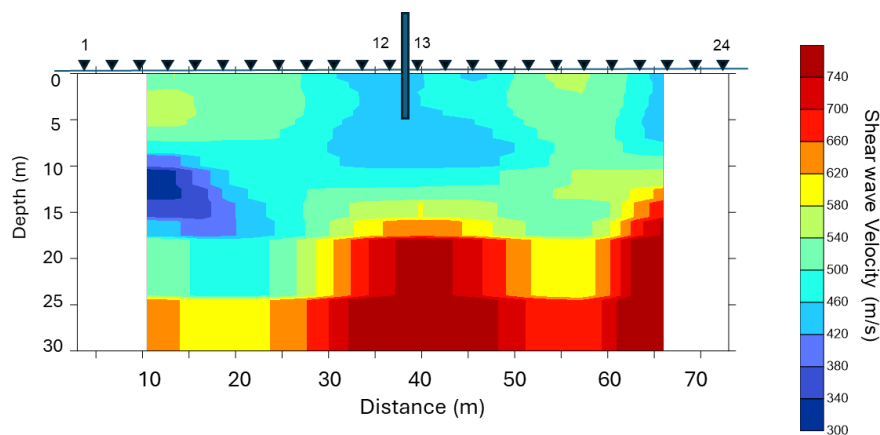


Figure 11 2-Dimensional depth profile illustrates the shear wave velocity distribution spatially and with depth around the drill, having stopped at 5 m.

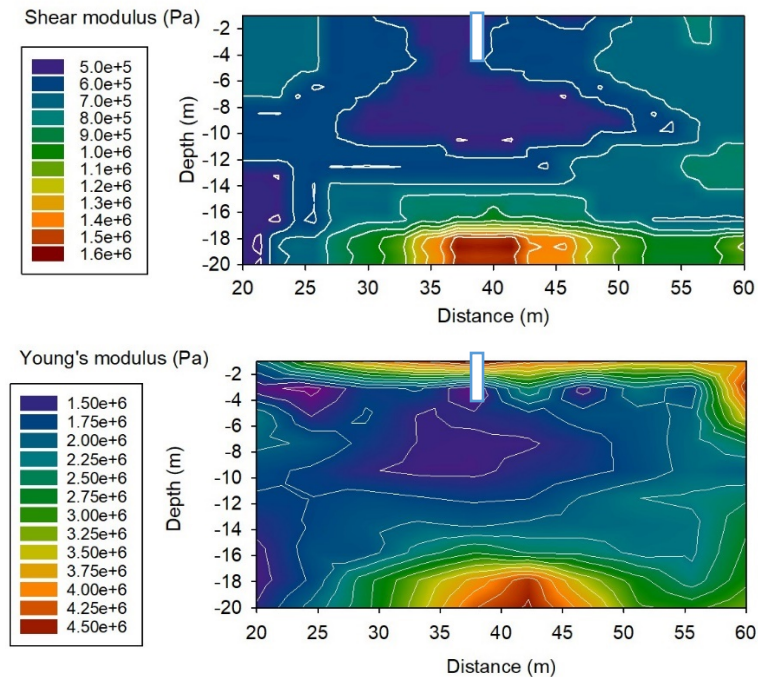


Figure 12 shows a 2-dimensional depth profile with stiffness profiles of Shear and Young's modulus interpreted from the shear-wave velocity profiles using an average density for sandy-silty-clay soils of 2.65 g/cm^3 . The white rectangle indicates the final drill position.

The results show the different processes occurring in the subsurface during the drilling, starting with initial compaction followed by what can be interpreted as fracture development and water infilling of the fractures. A deeper ground compaction has also occurred as a result of the drilling. The dynamic interaction of the drill with the surrounding soil can best be seen through a time-lapse sequence exhibiting changes in shear wave distribution spatially and at depth. This time sequence indicates the fluid particle-particle displacement, overall soil behaviour, and changes while drilling (see Figure 13).

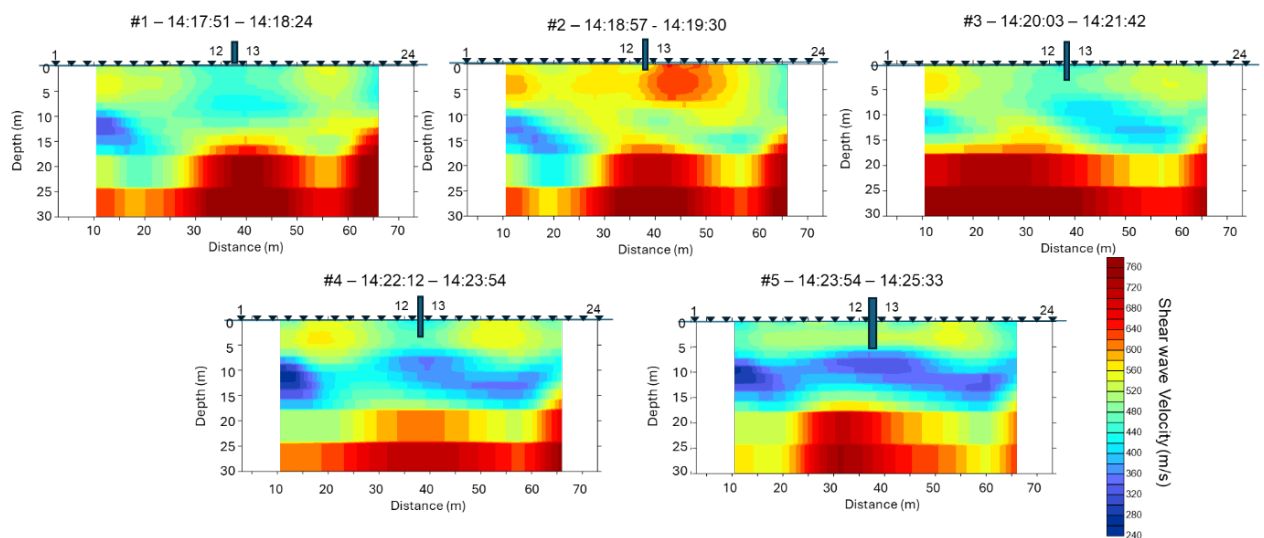


Figure 13 2-Dimensional shear-wave velocity time plots as the drilling takes place, with processing performed with 6 files of 10s for each time section.

4 CONCLUSIONS

The analysis of recorded waveforms showed a good sensitivity of S-waves to changes in geotechnical properties, e.g. compaction or water content, induced by the drilling process and the load of the micropile drill. The time-sequenced sample profiles show an impact of the drilling process and equipment on an area of up to 20 m laterally and depths up to ~15 m below the surface.

No significant changes were observed in the transmission of P-waves, as these are more associated with lithology and do not make them as suitable for imaging the impact of the drill. S-wave profiles, however, have shown good sensitivity to changes in the geotechnical properties of the soil, providing a high-resolution depth profile that can be used to image minor changes in soil compaction or water content of the formation. Increasing the azimuthal coverage and the aperture of the surveys, such as in the application of Acoustic Zoom's marine borehole seismics^{1,11} will provide good resolution, 4D imagery of the subsurface (time-lapse profiles, e.g., before, during, and after the drilling process), to fully interpret the impact of the drilling process and capture geotechnical values and behaviour on the surrounding sub-seabed.

5 REFERENCES

1. J.Y. Guigné and Machin, J.; System And Method For Determining Water Bottom Sediment Acoustic Properties Using A Pile Driver Acoustic Source, US Patent Filed in 2023
2. A.A. Oliner, ed; Acoustic Surface Waves. Springer. ISBN 978-3540085751; 1978
3. R.V. Goldstein, Gorodtsov, V.A.; Lisovenko, D.S.. "Rayleigh and Love surface waves in isotropic media with negative Poisson's ratio". *Mechanics of Solids*. 49 (4): 422–434; 2014
4. Jumrik Taipodia and Arindam Dey A Review of Active and Passive MASW Techniques, National Workshop, Engineering Geophysics for Civil Engineering and Geo-Hazards (EGCEG), 2012 CBRI,
5. Roorkee Gosar, A. Stopar, R. and Roser, J.; Comparative test of active and passive MASW methods and microtremor HVSR method, *Materials and Geo-environment*, 55, 41-66. 2008
6. J. N. Louie; Faster, better: shear-wave velocity to 100 meters depth from refraction microtremor arrays" *Bulletin of the Seismological Society of America*, 91, 347-364; 2001
7. C.B. Park, Miller, R.D., Xia. J. and Ivanov, J.; Multichannel analysis of surface waves (MASW)-active and passive methods, *The Leading Edge*; 2007
8. J.S. L'Hereux and Long, M; Relationship between Shear-Wave Velocity and Geotechnical Parameters for Norwegian Clays. *Journal of Geotechnical and Geoenvironmental Engineering*. Vol 143, No. 6; 2017
9. Tunusluoglu; Determination of empirical correlations between Shear wave velocity and penetration resistance in the Canakkale residential area (Turkey). *Applied Sciences*, vol 13, issue 17; 2023
10. P. Anbazhagan, Uday, A, Moustafa, S.S.R. and Al-Arifi, N.S.N.; Correlation of densities with shear wave velocities and SPT-N values. *Journal of Geophysics and Engineering*, vol 13; 2016
11. J.Y.Guigné, Stacey AJ, Clements C, Azad S, Pant A, Gogacz A, Hunt W, Pace NG; Acoustic Zoom high-resolution seismic beamforming for imaging specular and non-specular energy of deep oil and gas bearing geological formations, *J. Nat. Gas Sci. Eng.*, 21:568-591. doi:10.1016/j.jngse.2014.09.012; 2014